6 Special Techniques and Applications

6.1 Applications using Short Coherence Length Light

6.1.1 Light-in-Flight Measurements

Holographic recording of Light-in-Flight (LiF) was first proposed by Abramson [1-4]. He pointed out that a hologram can only image the distances in space where the optical path of the reference wave matches that of the object wave. The basic idea of LiF consists of recording a hologram of a plane object with streaking illumination by a short coherence length laser, figure 6.1. For this purpose a cw Ar-Ion laser without intracavity etalon is used. The coherence length of such laser is in the range of few millimeters or less. Alternatively also a picosecond pulsed dye laser can be used. The reference wave is guided nearly parallel to the holographic plate. In this way, only those parts of the object are recorded (and later reconstructed), for which the optical path difference (OPD) between object and reference wave is smaller than the coherence length of the light source. By changing the observation point in the developed plate, the above condition is met for different parts of the object, thus allowing observation of a wavefront as it evolves over the object.

Digital Holography has been applied to LiF recordings by Pomarico, Schnars, Hartmann and Jüptner [61, 126]. The general setup of figure 3.1 can be used for recording LiF if a short coherence length light source is used for illuminating the object. In the following investigations are described, in which an Ar-Ion laser pumped cw dye laser (Rhodamine 6G, λ = 574 nm) is used as light source. No frequency selecting elements are installed in the laser resonator. Therefore the output spectrum consists of many oscillating modes, resulting in a coherence length, which is determined by the LiF experiments to be 2.3 mm.

The laser beam is divided into a plane reference wave illuminating the CCD array and into a diverging wave illuminating the object, figure 6.2. The path differences are provided by glass plates with different but known thicknesses. The object consists of a plane aluminum plate of 2 cm × 2 cm area, the distance between object and CCD sensor is set to 1.67 m, and the angle of illumination α (referred to the normal of the object) is about 80 degrees. Furthermore, a wavelength of λ = 574nm is used and the maximum angle between object and reference wave is $q_{max} = 2°$. In this experiment a KODAK MEGAPLUS 4.2 camera with 2048 × 2048 light sensitive elements is used as recording medium.

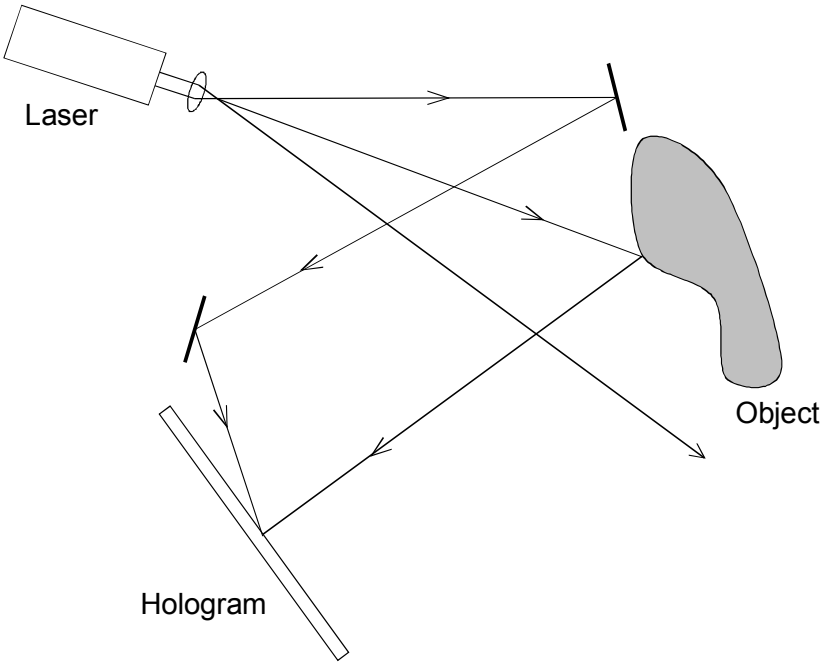

Fig. 6.1. Light-in-flight holography

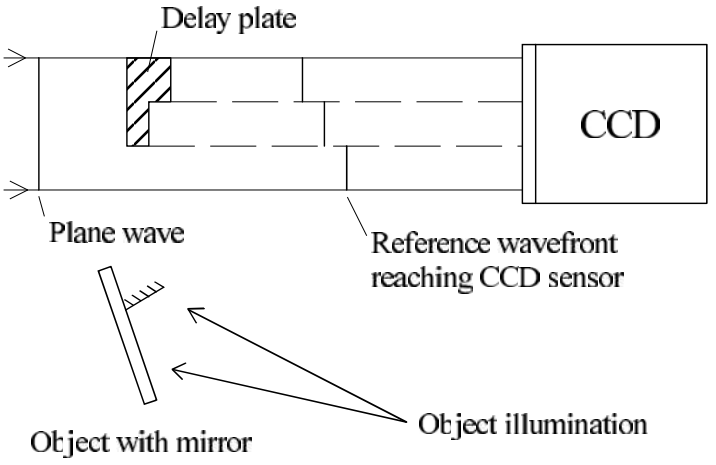

Fig. 6.2. Optical set-up for Digital LiF recording with delay lines by glass plates

The first experiment is performed without the glass plates in the reference arm of the interferometer. Since the object is illuminated under an angle only a part of the object could be illuminated in coherence to the reference wave. The numerical

reconstruction of such a digitally recorded hologram shows, as expected, a bright stripe representing the wavefront, figure 6.3.

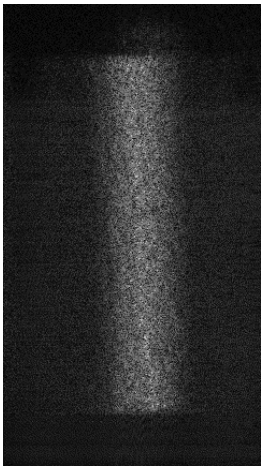

Fig. 6.3. Numerically reconstructed wavefront

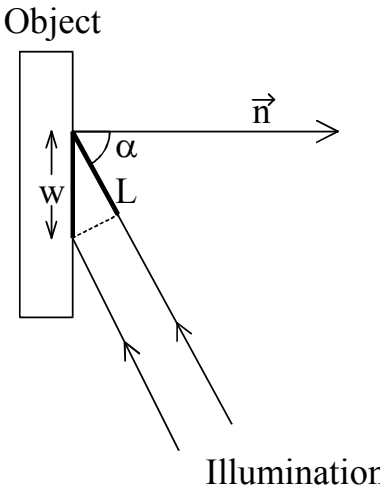

Fig. 6.4. Geometrical considerations for calculating the coherence length

The reconstructed image is available in a digital form and further processing is easy to be done. For example, the coherence length can be calculated from this image, figure 6.4. The width of the bright stripe (wavefront) seen at the object is determined from both, the coherence length of the light source, *L*, and the geometrical conditions of the holographic set-up. If a plane reference wave is used and

the angle between the interfering waves is small ($q_{\max} = 2°$ in this example), only changes in the optical path due to the illumination beam have to be considered. In this case the bright zone at the object has a width w given by

$$w = \frac{c\tau}{\sin\alpha} = \frac{L}{\sin\alpha} \tag{6.1}$$

where α is defined in figure 6.4 and τ is the coherence time. After measuring w, Eq.(6.1) can be used to calculate the coherence length L of the light source using the known angle α of the incident wave. As the measurements of the width are disturbed by electronic and coherent noise, direct measurement of the intensity profile leads to errors. A good result can be achieved by low-pass filtering of the image and by applying the autocorrelation function to the intensity profile line. The width of the wavefront measured by this procedure values to 45 pixels. The experimental conditions are:

$\Delta x = 9\mu m$; $d = 1.67m$; $\lambda = 574nm$; $\alpha = 80°$

The resulting coherence length is therefore

$$L = w\sin\alpha = 45 \cdot \Delta\xi \sin\alpha = 2.3mm \tag{6.2}$$

where Eq. (3.23) is used for calculating the image resolution $\Delta\xi$.

It is also possible to apply Digital Holography to follow the evolution of a wave front in its "flight" over an object, as proposed in the original work of Abramson for conventional holography. However, because of the reduced size of the CCD target and the lower resolution compared to a holographic plate, only slightly different points of view of the wave front can be registered in each hologram. Some view-time expansion is also needed.

A possible setup for this purpose, using a skew reference wave, has been proposed by Pettersson et.al. [125]. Yet, this solution cannot be applied here because the high spatial frequencies that would be produced at the sensor are not resolvable. A solution to this problem is to record a hologram introducing different phase delays in different parts of the plane reference wave. That can be achieved e.g. by introducing plane-parallel plates of different thickness in the plane wave illuminating the CCD sensor, figure 6.2. A plate of thickness p and refraction index n will produce a delay Δt with respect to air (or the vacuum with light speed c) given by:

$$\Delta t = (n-1)\frac{p}{c} \tag{6.3}$$

That way it is possible to record at one time several holograms of the object using a corresponding number of reference waves delayed with respect to each other. The numerical reconstruction can be done for each part of the CCD array in which the phase of the reference wave has a particular delay, giving rise to the desired "times of evolution" of the wave front illuminating the object. This is equivalent to choose another observation point in the original LiF experiment. In this sense, the phase delays introduced in the different parts of the reference wave can

be interpreted as artificial extensions of the CCD sensor and allow a better visualization of the phenomenon.

In the experiments 6 mm thick PMMA plates (refraction index n ~ 1.5) are used to produce the phase delays in the reference wave, figure 6.2. One third of the original plane reference wave does not travel through PMMA, the second third, illuminating the sensor in the middle, travels through 6 mm PMMA (representing 10*ps* delay with respect to air) and the last third travels through 18mm PMMA (30*ps* delay with respect to air). The object as seen from the CCD sensor is schematically sketched for better recognition of the results, figure 6.5. It consists of a 3cm × 3cm plane aluminum plate, which was painted matt white for better light scattering. A small plane mirror (1cm × 1cm area) is attached to the plate, perpendicular to its surface and at an angle of about 10 degrees away from the vertical.

The three reconstructed stripes of the hologram, corresponding to three different times of evolution of the wavefront illuminating the object are shown in figure 6.6. One part of the wavefront is reflected by the mirror, the other part is traveling in the original direction. The three pictures can be interpreted as a slow-motion shot of the wavefront. As demonstrated before, quantitative results can be derived from these images, e.g. the speed of light.

The minimum number of pixels required for a part of the hologram to be successfully reconstructed limits the number of different "times of evolution" that can be recorded simultaneously . Furthermore, due to the borders of the plates introduced in the reference wave diffraction effects cause dark zones at the CCD which cannot be used for numerical reconstruction.

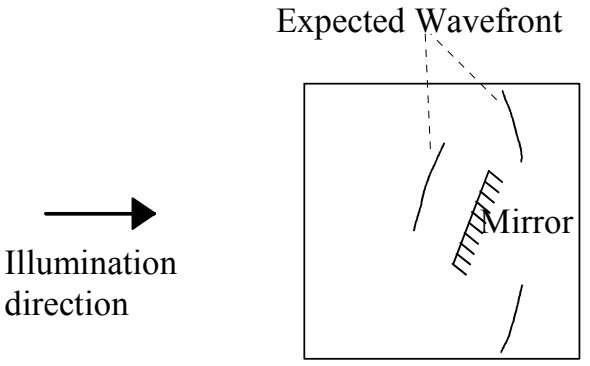

Fig. 6.5. Object used for displaying the temporal evolution of a wave front as seen from the CCD sensor

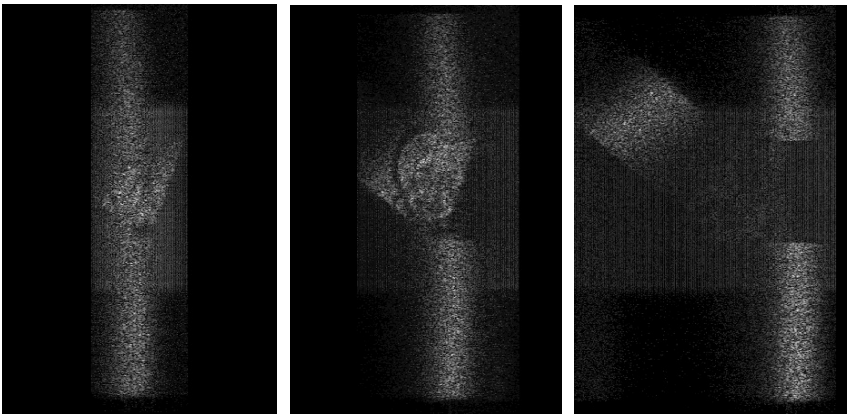

Fig. 6.6. The wavefront at three different times, reconstructed from one single holographic recording.
Left: No delay, wavefront just reaching mirror.
Middle: 10 ps delay, the mirror reflects one part of the wavefront.
Right: 30 ps delay with respect to the left recording, one part is reflected into the opposite direction, the other part is traveling in the original direction

6.1.2 Short-Coherence Tomography

The main disadvantage of introducing the path differences by glass plates with different thickness are the diffraction effects at the edges of the plates. Therefore this technique allows only a few discrete depth steps. To overcome this problem, Nilsson and Carlsson proposed to use a blazed reflection grating for generating path differences [13, 101-103]. The set-up is composed of a Michelson Interferometer, figure 6.7, in which one mirror is replaced by the grating. The incoming beam of a light source with sufficient short coherence length is split into two partial beams. One partial beam illuminates the object and is diffusely reflected from the surface to the CCD. The other beam is guided to the blazed reflection grating. The grating retro reflects that beam back into the opposite direction to the incident beam, introducing a spatially varying delay across the beam profile. Both beams interfere at the CCD, which records the hologram. The method can be applied to measure the three-dimensional object shape. This is possible because each vertical stripe of the hologram fulfils the coherence condition for different object depths. Reconstructions from different hologram parts create different depth layers of the object.

Instead of the grating in figure 6.7 it is also possible to use an ordinary mirror in the reference arm, see e. g. [117], which can be shifted in the direction of beam propagation. Digital holograms are then recorded in different mirror positions. Each single hologram represents another depth layer of the object and the shape can be calculated from the holographic reconstructions. However, there is an advantage of the setup shown in figure 6.7 using the grating: Only one recording is necessary to determine the whole shape.

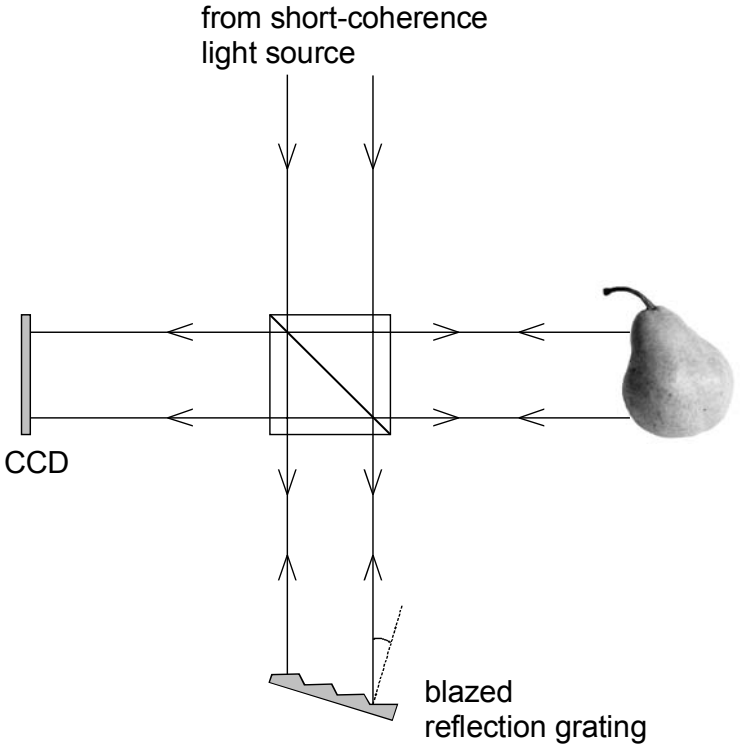

Fig. 6.7. Short-coherence length tomography using a blazed grating

6.2 Particle Distribution Measurements

The size, the speed, and the distribution of particles within fluid or gaseous media are measured with optical techniques like laser-doppler-anemometry (LDA), phase-doppler-anemometry (PDA) or particle image velocimetry (PIV). To achieve the three-dimensional spatial distribution of particles also holographic techniques are used, see corresponding articles of Trolinger [161] or Hinsch [49]. However, the development of the exposed hologram (photographic plate) and the evaluation of the distribution of the droplets are time consuming processes. Digital Holography where holograms are recorded with the CCD-sensor followed by numerical reconstruction of the object wave offers new alternatives.

Digital holograms of particle distributions within transparent media can be recorded with the simple in-line set-up depicted in figure 6.8. A plane wave illuminates the observed particles. A part of the wave is diffracted by the particles while the remaining part passes through the set-up without being diffracted. This part of the wave serves as a reference wave. The waves interfere and produce a typical diffraction pattern on a CCD-sensor.

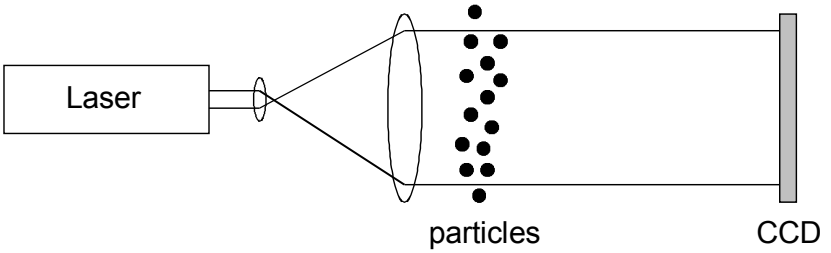

Fig. 6.8. In-line set-up

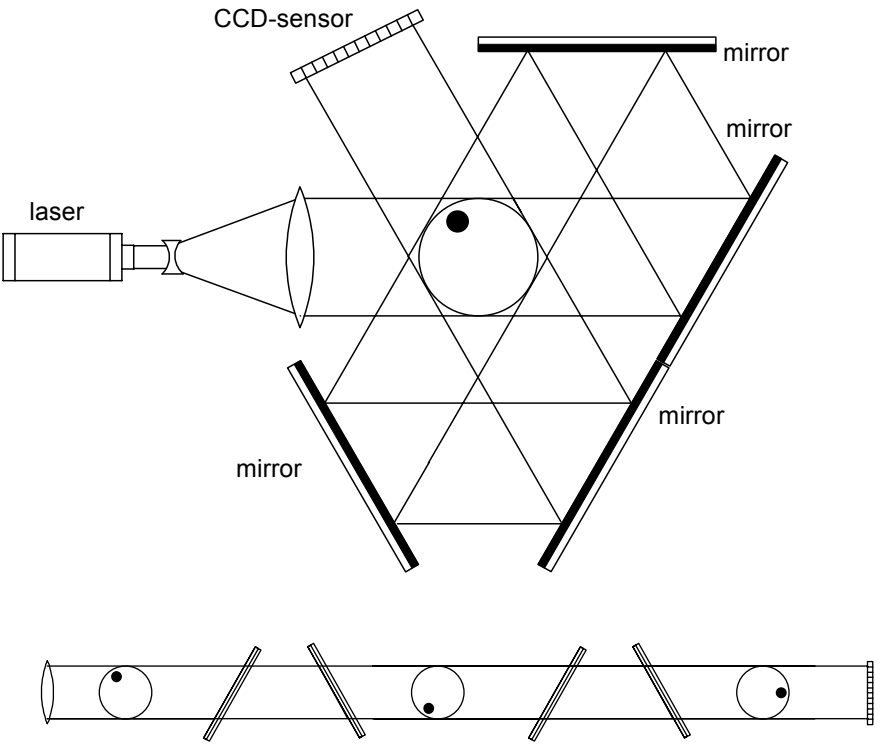

Fig. 6.9. Experimental set-up for recording in-line holograms from several directions with one CCD-sensor and deconvoluted lightpath (from [5])

The three-dimensional spatial distribution of small moving particles - their size and their position - can be detected by scanning the reconstruction distance in the computer: Since in numerical reconstruction the distance d may be chosen freely, the field can be scanned by varying d and check at which distances the particles are in focus.

The depth of focus in holographic imaging is a function of reconstruction distance d, wavelength λ and the aperture of the hologram. In Digital Holography the aperture is the CCD. In a typical example using a CCD with 18mm × 18mm area, a wavelength of λ=692nm (pulsed ruby laser) and an average reconstruction distance of d=0.5m the focal depth is in the range ±0.5mm. But due to the slow decrease of sharpness outside this range objects could only be detected with a positional uncertainty of about ±1cm.

In order to enhance the depth resolution, Kreis et. al. combined Digital Holography with tomographic methods [5, 6, 77]. In tomography a manifold of projections in different directions through a scene are recorded. The three-dimensional distribution of the physical quantity, e.g. the attenuation of a beam passing the scene, is then calculated by numerical methods.

To record simultaneously multiple in-line holograms of the particle stream an arrangement using a single CCD-array has been designed. After passing the particles a first time the collimated beam of a ruby pulse laser is guided by two mirrors to a second pass and by two further mirrors to a third pass through the stream before hitting the CCD-sensor. Fig. 6-9 shows schematically the dislocation of the mirrors and the deconvoluted light path. Now it is possible to extract the three views of the particles by three reconstructions with numerical focusing to the different distances. In the realized set-up the reconstruction distances are 40 cm, 65.5 cm and 95.5 cm.

The set-up is used to analyze the particle stream by Digital Holography and tomographic methods. The particles with a size of 250 µm are sprinkled manually. The diffracted light is recorded with a CCD-sensor which consists of 2048 × 2048 light-sensitive pixels. The pixel distance is 9 µm × 9 µm. The diffraction rings of each particle can be recognized in the recorded diffraction pattern (in-line hologram), figure 6.10. The more the distance of the particles to the CCD-sensor increases, the more the spacing among the concentric rings belonging to an individual particle increases as well. In addition to the diffraction rings caused by the particles, the image is overlapped with a pattern produced by the recording system itself. For protection from damage and dust, a thin glass plate covers the CCD-sensor. If illuminated with coherent light the plate produces an interference pattern. This interference pattern is even visible, if the CCD-sensor is illuminated with a plane wave and no particles are observed.

The reconstructed particles are visible as dark spots without any diffraction rings, figure 6.11. The missing diffraction rings or at least halos show that the particles are reconstructed with the appropriate distance. The lateral resolution in the reconstructed images is 9µm. The measured average particle diameter is 28 pixels, corresponding to 261µm.

The three reconstructed images show the particle stream from different directions. To gain a three-dimensional particle distribution from these images, a tomographic method is applied, Fig. 6-12.

From every image in figure 6.12 a line is taken and from the three lines a two-dimensional profile through the particle stream is calculated with a method based on the filtered backprojection approach of tomography. If this method is applied

for all lines in the reconstructed images, a full three-dimensional distribution of the particles is achieved.

The three back projections of one particle must be in one plane. In the crossing of the three stripes a particle is reconstructed. The stripes arise from the low number of views used in the tomographic evaluation. With increasing number of views the stripes begin to disappear.

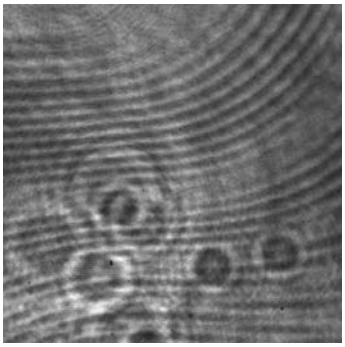

Fig. 6.10. In-line hologram, recorded from particles with a size of 250 μm at a distance of 40 cm, 65.5 cm and 95.5 cm

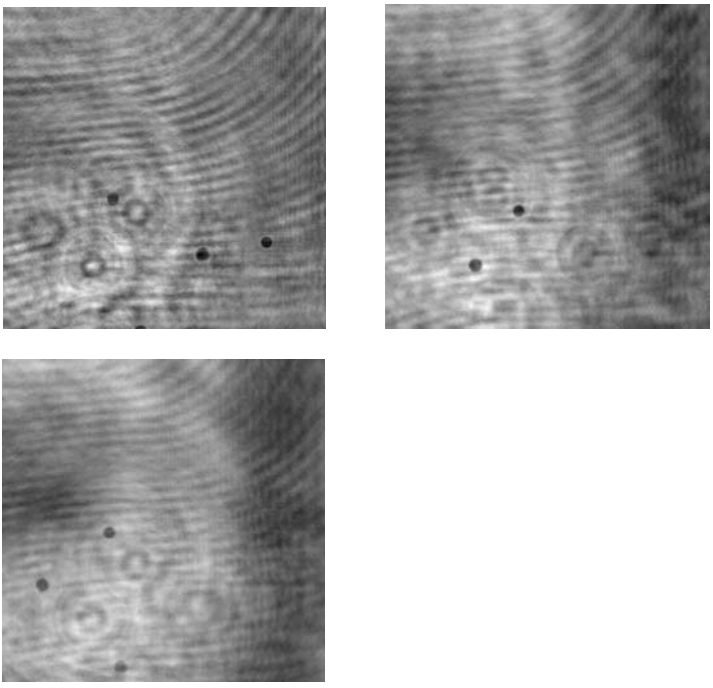

Fig. 6.11. Reconstructed particle distributions at a distance of 40cm, 65.5cm and 95.5cm.

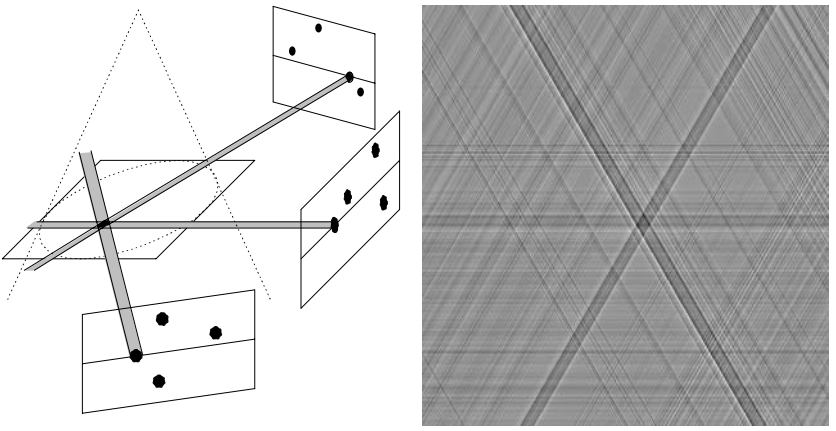

Fig. 6.12. *Left:* Principle of tomography. From the existing images single lines are taken and combined to a two-dimensional distribution by methods of tomography. *Right:* Two-dimensional distribution gained from three different views. In the crossing of the stripes a particle is found (from [5]).

6.3 Endoscopic Digital Holography

Digital Holography provides the possibility to combine deformation measurement and surface contouring in one single set-up. For measuring the object deformation in the simplest case two holograms with a certain wavelength have to be recorded for different object states (chapter 4.2). For shape measurement the object has to remain unchanged while two holograms with slightly different wavelengths or slightly different illumination points are recorded (chapter 4.3). Thus, and due to the relative simple set-up this method appears to be well suited to endoscopic measurements. It is obvious that the requirements for an endoscopic Digital Holography sensor are much higher than they are for a laboratory breadboard. Compared to a laboratory set-up the endoscopic system has to be

- more flexible;
- robust against harsh environments;
- faster in data processing;
- very small;
- adapted to restrictions caused by the system size;
- user friendly.

A sketch of a developed prototype system is shown in figure 6.13, while figure 6.14 depicts a functional prototype of the sensor head. The system can be divided in four parts: The controlling computer, the laser and the corresponding fibre coupling units, the endoscope and the sensor.

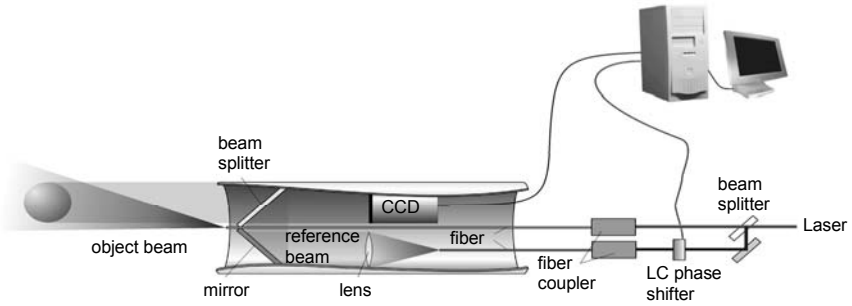

Fig. 6.13. Sketch of an endoscope based on Digital Holography

Fig. 6.14. Sensor head of the endoscope (photo: BIAS)

The sensor head has a diameter of 15 mm (current stage). For the future it is intended to decrease the size to a diameter of less than 10 mm.

The heart of the sensor is a commercial miniature CCD-camera with a 1/3'' CCD-matrix. Including the housing, this camera has a diameter of 10 mm. The objective of the camera is removed to be able to record the digital holograms. Since the camera provides a standard video-signal the hologram can be grabbed by a conventional frame grabber. For the object- and the reference beam mono-mode glass fibres are used. Currently, a single illumination beam is utilized. This is sufficient to measure the shape of the object and to measure one displacement component – in our case the out-of-plane component. However, in the next step three illumination directions will be implemented to be able to perform a 3D displacement measurement.

In general every laser source with sufficient coherence length can be used for deformation measurements. However, the wavelength of the laser has to be tuneable for shape measurements. Thus, to keep the whole system portable, currently a VCSEL laser diode is used as a light source. The wavelength for this laser diode

type can be tuned continuously in a range of about 8 *nm*. Unfortunately, VCSEL laser diodes have a very low output power (0.5 mW @ 760 nm for single mode emission). That is why this light source can only be used for highly reflecting objects.

From figure 6.13 it can be seen that the laser beam passes through a liquid crystal phase shifter before it is coupled into the fibre for the reference beam. This LC phase shifter is used to record temporal phase shifted holograms. A simple reconstruction without using phase shifting methods results in an image that contains the desired object image and additionally the twin image together with the zero order term. By using the method of temporal phase shifting the conjugate image as well as the zero order can be eliminated completely from the resulting image (see chapter 3.3.3). In this way the entire CCD-target can be used for the measurement, i.e. the full space bandwidth of the CCD can be utilized. This is of great importance, since the choice of the camera is restricted by the system size. Cameras of this size are only available with a limited pixel number, which makes it necessary to make use of the full sensor size.

The high sensitivity of Digital Holography to object motions is also a disadvantage for a system that is intended to be used outside the laboratory. Even small object vibrations caused by environmental influences can disturb the measurement. The effect of those disturbances can be minimised by decreasing the time needed for a measurement. Thus, a high processing speed and a fast data acquisition are important to minimize the influence of unwanted vibrations. In order to achieve a high processing speed of the holograms an optimized phase-shift algorithm has been chosen [87]. More than six reconstructions per second are possible for holograms with 512 x 512 pixels using a common PC with 1.4 GHz clock frequency.

Another benefit of a high processing speed is the possibility to unwrap the phase maps of deformation measurements in real time by temporal phase unwrapping [53]. In this method the total object deformation is subdivided in many measurement steps in which the phase differences are smaller than 2π. By adding up those intermediate results, the total phase change can be obtained without any further unwrapping. This is an important feature, since it is essential to have an unwrapped phase to be able to calculate the real deformation data from the phase map. Fig. 6.15 shows an example of such a measurement. The left image shows the wrapped deformation phase for a clamped coin which was loaded by heat. The right image shows the temporal unwrapped phase, which has been obtained by dividing the total deformation in 85 sub-measurements.

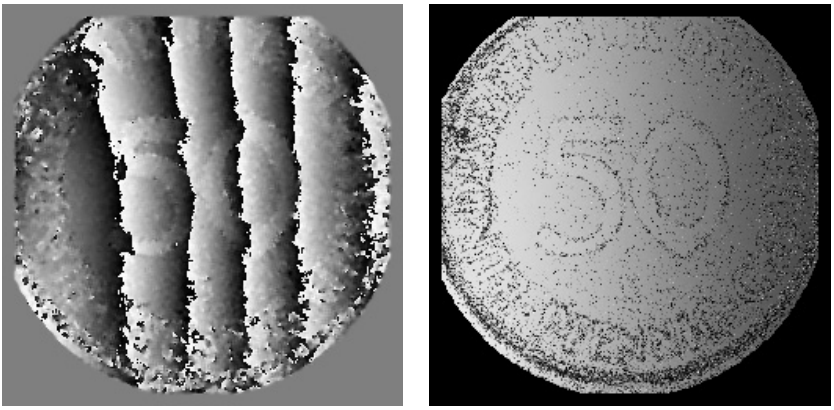

Fig. 6.15. Wrapped deformation phase of a heat loaded coin (left) and unwrapped phase generated by temporal unwrapping (right)

6.4 Optical Reconstruction of Digital Holograms

The techniques discussed in this chapter differ from the other methods described in the previous chapters, because the reconstruction is performed with an optical set-up. A computer is just used as intermediate storage medium for digital holograms.

Liquid Crystal Displays (LCD's) are electro-optical devices used to modulate light beams. Likewise they can be used as a spatial light modulator for holography. An individual LCD cell changes its transmittance depending on the applied voltage. It is therefore possible to modulate the brightness of light, which passes the device.

Optical hologram reconstruction with a LCD is possible e. g. with the set-up of figure 6.16. At first a digital hologram is recorded with a CCD-sensor, figure 6.16(a). The hologram is stored and then transmitted to the reconstruction set-up, figure 6.16(b). Recording and reconstruction set-ups could be located at different sites. The LCD modulates the reconstruction beam with the hologram function. The original object wave is reconstructed due to the diffraction of the reconstruction beam at the modulated LCD. The virtual image can be observed at the position of the original object. Usually a CCD-camera is used to record the image. Alternatively it is possible to reconstruct the real image by illuminating the LCD with the conjugate reference wave.

An example of such an optical reconstruction of a digitally recorded hologram is shown in figure 6.17(a). A digital hologram of a knight is recorded and stored. The image of the knight becomes visible if the LCD with the hologram mask is illuminated by a reconstruction wave. Optical reconstruction of two superimposed holograms, which are recorded in different object states results in a holographic interferogram, figure 6.17(b).

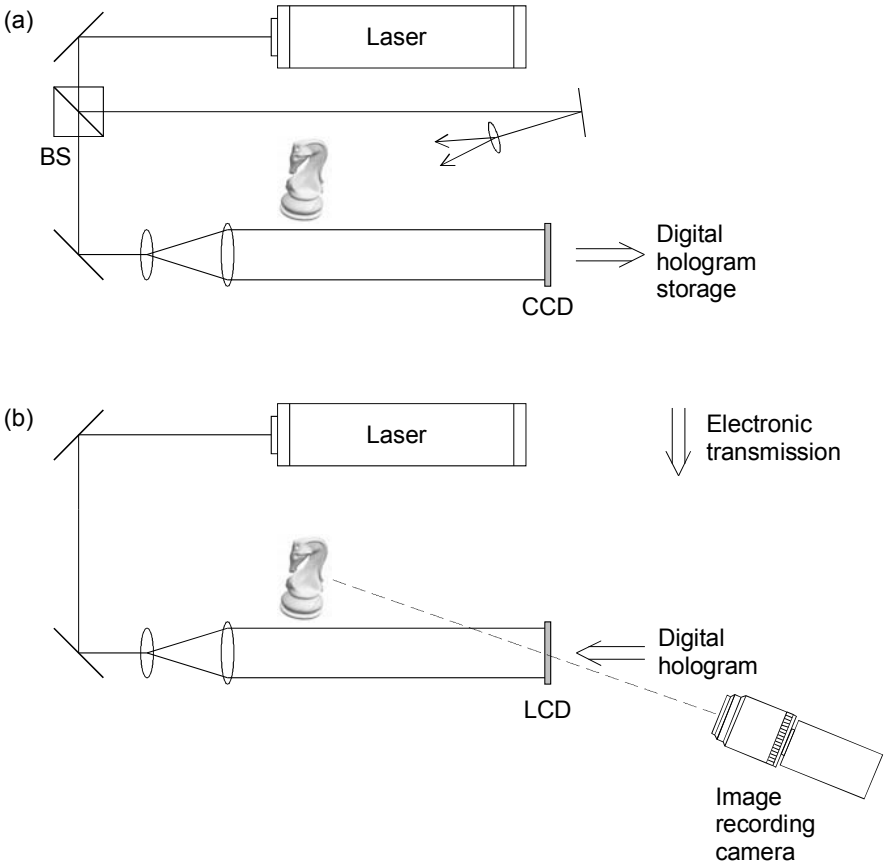

Fig. 6.16. (a) Digital hologram recording with a CCD
(b) Optical reconstruction with a LCD

Instead of a LCD other electro-optical devices can be used as spatial light modulators, too. Recently Kreis, Aswendt und Höfling published the optical reconstruction by means of a Digital Mirror Device (DMD) [78]. A DMD is a silicon micromachined component, which consists of an array of tiltable aluminium mirrors mounted on hinges over a CMOS static random access memory (SRAM). Today DMD's are available with up to 1280 × 1024 mirror elements. The individually addressable mirrors can be tilted binary either –10 *deg* (on) or +10 *deg* (off) along an axis diagonal to the micromirror. In an optical reconstruction set-up DMD's are therefore operated in reflection. In contrast to LCD's, which absorb up to 90% of the available light, a DMD is a reflective device yielding much more light. Consequently the diffraction efficiency in the hologram reconstruction is better compared to LCD's.

A very simple device for displaying digital holograms is a computer printer. The high resolution of standard ink-jet or laser printers with up to 3000 dots per inch makes it possible to print digital holograms directly on a transparent film. The hologram is then reconstructed by illuminating this film with the reconstruction wave.

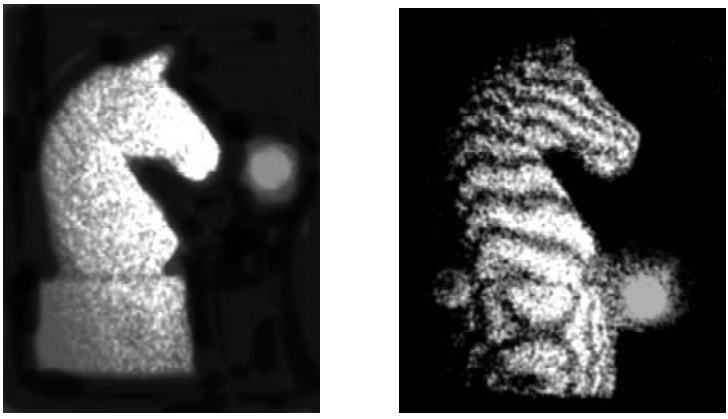

Fig. 6.17. (a) Optical reconstruction of a digital hologram by means of a LCD (b) Optically reconstructed holographic interferogram (from [111])

6.5 Comparative Digital Holography

6.5.1 Fundamentals of Comparative Holography

The essential of interferometry is the comparison of the optical wave reflected or transmitted by the test object with another, known wave field. In Holographic Interferometry at least one of these waves is stored by a hologram. By interference the phase differences between the two wave fields can be measured. The phase differences are connected to the quantities to be determined by the geometry function of the set-up. In this way it is possible to measure e.g. shapes or deformations of technical objects. However, a severe restriction in conventional HI is that interference is only possible, if the microstructures of the surfaces to be compared are identical. The change of the surface by the exchange of the object or e.g. too high deformations leads to a decorrelation of the two speckle fields and the loss of the interference. Thus standard HI is restricted to the comparison of two states of the *same* object.

A method to overcome this restriction is comparative interferometry [36, 100]. This method is based on the illumination of the two states of the test component with the corresponding conjugated object wave of the master object: The object wave of the master component acts as a coherent mask for the adaptive illumination of the test component.

Comparative interferometry is performed according to the following principle: At first a double exposure hologram of the master object is taken in the two states according to a specific load. The reconstruction of this double exposed hologram generates an interferogram. The relation between the measured interference phase and the displacement vector is given by Eq. (2.84):

$$\Delta\varphi_1(x,y) = \frac{2\pi}{\lambda}\vec{d}_1(x,y,z)\left(\vec{b}_1 - \vec{s}_1\right) = \vec{d}_1\vec{S}_1 \tag{6.4}$$

The test object is investigated in a modified set-up for comparison with the master: It is illuminated in the original observation direction $\vec{b}_1$ by the reconstructed, conjugated wave front of the master object, i.e. the real image of the master object is projected onto the test object. It is observed in the original illumination direction $\vec{s}_1$. This results in

$$\vec{s}_2 = -\vec{b}_1 \qquad \text{and} \qquad \vec{b}_2 = -\vec{s}_1 \tag{6.5}$$

$$\Delta\varphi_2(x,y) = \frac{2\pi}{\lambda}\vec{d}_2(x,y,z)\left(\vec{b}_2 - \vec{s}_2\right) = \frac{2\pi}{\lambda}\vec{d}_2(x,y,z)\left(\vec{b}_1 - \vec{s}_1\right) \tag{6.6}$$

Since the test object is illuminated by the conjugated wave front of the master the interferogram indicates the difference of the displacements between the two objects:

$$\Delta\varphi(x,y) = \Delta\varphi_1(x,y) - \Delta\varphi_2(x,y) = \frac{2\pi}{\lambda}\left(\vec{d}_1(x,y,z) - \vec{d}_2(x,y,z)\right)\left(\vec{b}_1 - \vec{s}_1\right) \tag{6.7}$$

6.5.2 Comparative Digital Holography

Comparative Digital Holography is a combination of comparative holography with Digital Holography [111-112]. The set-up for comparative Digital Holography follows the principle of Digital Holography and adapts the comparative method, figure 6.18. The digital hologram of the master object is recorded at a location A, figure 6.18(a). The transmission of this digital hologram to a test location B can be done by any data transfer medium, e.g. by the internet. At location B the hologram is fed into a Liquid Crystal Display as spatial light modulator. A laser reconstructs the hologram optically.

For the comparative holography the conjugated wavefronts of the master object are reconstructed and illuminate the test object, figure 6.18(b). The observation is done in the original illumination direction. A great advantage of comparative Digital Holography compared to conventional comparative HI is, that the holograms of all states can be stored and later reconstructed separately from each other. Therefore no additional reference waves are needed for the separate coding of the different holograms. This characteristic of Digital Holography reduces the technical requirements for comparative measurements significantly.

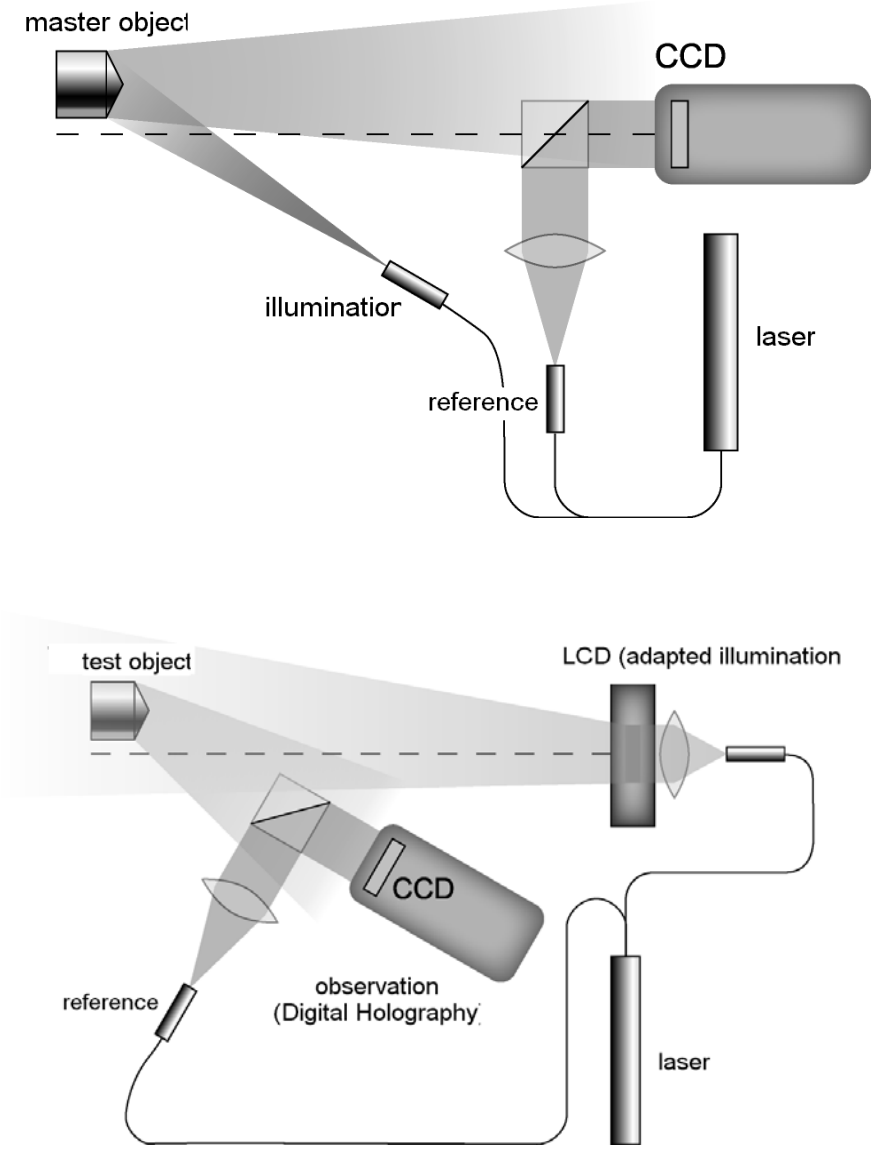

Fig. 6.18. Comparative Digital Holography (from [111])
(a) Recording of the mask
(b) Coherent illumination of the test object with the conjugated wavefront of the master

The method is demonstrated by the determination of a small dent in one of two macroscopically identical cylinders with cones at their upper end. The depth of the dent is about a few micrometers. With holographic two-wavelength contouring, the observed phase differences can be described by

$$\Delta\varphi_1(x,y) = \frac{2\pi}{\Lambda}\left(\vec{b}_1 - \vec{s}_1\right)\overrightarrow{\Delta r}_1(x,y) \tag{6.8}$$

$$\Delta\varphi_2(x,y) = \frac{2\pi}{\Lambda}\left(\vec{b}_2 - \vec{s}_2\right)\overrightarrow{\Delta r}_2(x,y) \tag{6.9}$$

The indices 1 and 2 mark the master or the test object, respectively. Λ is the synthetic wavelength. The measurements are carried out with Λ = 0,345 mm (λ_1 = 584,12 nm and λ_2 = 585,11 nm). $\overrightarrow{\Delta r}_1$ and $\overrightarrow{\Delta r}_2$ represent the relative height deflection of the master resp. the test object. Figure 6.19(a) shows the reconstructed intensity of the test object, while the mod2π contour lines are depicted in figure 6.19(b). The dent is hardly to recognize. However, after holographic illumination of the test object with the real image of the master, the difference phase $\Delta\varphi$ corresponds to the difference in height deflections between master and test object:

$$\Delta\varphi(x,y) = \Delta\varphi_1(x,y) - \Delta\varphi_2(x,y) = \frac{2\pi}{\Lambda}\left(\overrightarrow{\Delta r}_1(x,y) - \overrightarrow{\Delta r}_2(x,y)\right)\left(\vec{b} - \vec{s}\right) \tag{6.10}$$

This phase difference is shown in figures 6.19c (mod2π-map) and 6-18d (pseudo 3D-map).

The measured phase difference distribution is quite noisy because of the large pixel sizes of the CCD target and the spatial light modulator (CCD: 9 μm, LCD: 29 μm). In the future better optical components might be available. Nevertheless, the comparison of figures 6.19b with 6-19d demonstrates the advantage of comparative Digital Holography to measure the shape difference of two objects with different microstructure: in the phase difference image the dent is clearly recognizable.

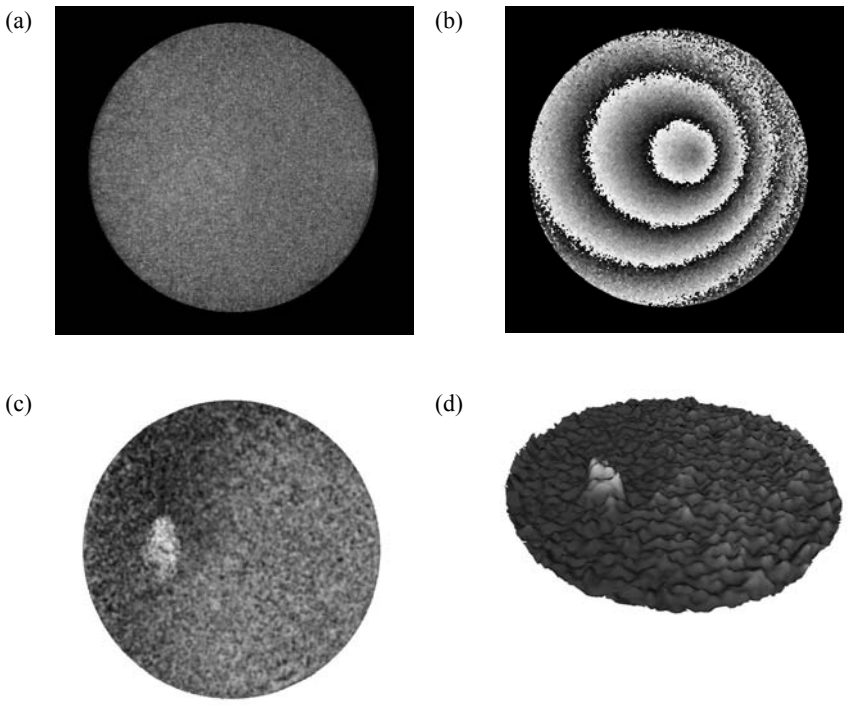

Fig. 6.19. Demonstration of comparative Digital Holography (from [112])
(a) Reconstructed intensity, test object
(b) Phase contour lines, test object
(c) Comparative phase difference, mod2π-map
(d) Comparative phase difference, pseudo 3D-map

6.6 Encrypting of Information with Digital Holography

The reconstruction of objects from their holograms is only possible, if the reconstruction wave has nearly the same properties like the reference wave used in the recording process. Any deviation from the original amplitude and phase distribution results in image aberrations or in total loss of the original object information. The reference wave used for hologram recording can be therefore regarded as a key to reconstruct the information coded in the hologram. This is the principle of information encryption by holography.

In the following a coding method proposed by Javidi et. al. [56, 155, 156] is described. The method is based on phase-shifting Digital Holography, see set-up in figure 6.20. The key for encrypting the information is a diffusely scattering screen. At first the key is recorded holographically. A parallel beam is split into two coherent partial beams at beam splitter BS1. One partial beam illuminates the screen from the back.

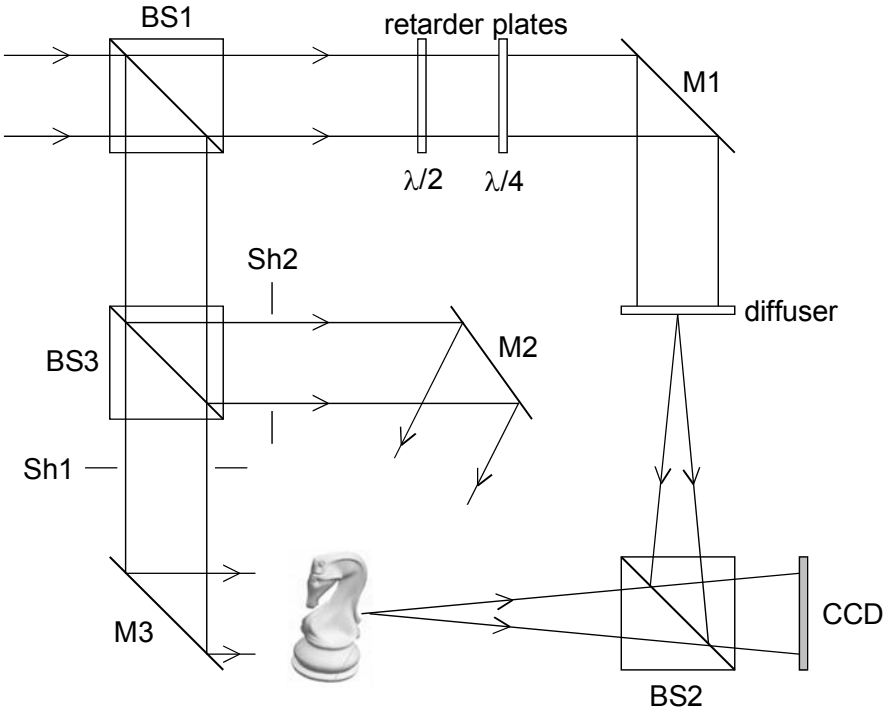

Fig. 6.20. Information encrypting with Digital Holography

The scattered light is guided to the CCD via beam splitter BS2. The other beam is guided via BS3, mirror M3 and BS2 to the CCD. For this shutter SH1 is opened, shutter SH2 is closed and the object is removed. Both beams interfere at the surface of the CCD. A set of four interferograms with mutual phase shifts is recorded by means of phase shifting devices. This can be done either by aligning the fast and the slow axes of optical retarders with the polarization of the incident beam (as shown in figure 6.20) or by other electro-optical devices like piezo electric driven mirrors. The complex amplitude of the plane partial wave guided via mirror M3 is $1 \cdot e^{i \cdot 0}$ in the simplest case. Consequently, it is possible to calculate the complex amplitude $a_K e^{i\varphi_K}$ of the wave scattered from the diffuser in the CCD plane by phase shifting algorithms (see also chapter 2.7.5). If four interferograms I_1 to I_4 with equidistant phase steps of $\pi/2$ are recorded the amplitude and the phase of the "key" wave are determined by following equations:

$$\varphi_K = \arctan \frac{I_4 - I_2}{I_1 - I_3} \tag{6.11}$$

$$a_K = \frac{1}{4}\sqrt{(I_1 - I_3)^2 + (I_4 - I_2)^2} \tag{6.12}$$

Now a hologram of the object to be encrypted is recorded. For this shutter SH1 is closed, and shutter SH2 is opened illuminating the object via M2. The scattered light from the screen is now used as reference wave. Again a set of four phase shifted interferograms I_1' to I_4' is generated. The difference phase between the "key" wave phase φ_K and the object phase φ_0 is determined by:

$$\varphi_0 - \varphi_K = \arctan\frac{I_4' - I_2'}{I_1' - I_3'} \tag{6.13}$$

The following equation is valid for the product of the amplitudes:

$$a_0 \cdot a_K = \frac{1}{4}\sqrt{(I_1' - I_3')^2 + (I_4' - I_2')^2} \tag{6.14}$$

Without knowledge of a_k and φ_K it is obviously not possible to calculate the complex amplitude of the object wave in the CCD plane. The object can only be reconstructed with the numerical methods described in chapter 3, if the correct key is given. This key consists of amplitude and phase of the wave scattered from the diffuser. A second key, which has to be known for correct object decoding, too, is the recording distance d between diffuser and CCD.

6.7 Synthetic Apertures

Every part of a hologram contains the entire object information. The object can be reconstructed therefore from any cut-out of the hologram, the size of such a cut-out only influences the speckle size in the reconstructed image. On the other hand it is also possible to synthesize a hologram from different single holograms [79]. A possible recording geometry with two CCD's is depicted in figure 6.21 for a plane reference wave. Independent CCD-cameras are used to record the single holograms. A fixed phase relation between the individual holograms is ensured by using the same reference wave. Reconstruction of the synthesized hologram is possible by following methods: The single holograms are reconstructed separately and the resulting complex amplitudes in the image plane are coherently superimposed. A second possibility is to embed both single holograms in an artificial large hologram, where the grey values of all pixels not covered are set to zero (black). Such artificial hologram matrix is then reconstructed as a whole.

The resolution of images and phase maps reconstructed from digital holograms depends on the recording distance d and on the effective aperture $N\Delta x$, see Eq. (3.23). However, both quantities are not independent from each other, because for state of the art CCD's with pixel sizes in the range of $5\mu m$ large apertures require also long recording distances due to the spatial frequency limitations discussed in

chapter 3.4.2. Increasing the aperture size by using more than one CCD therefore does not automatically improve the image resolution, because the larger synthetic aperture requires a longer recording distance. In order to decouple recording distance and aperture size it is therefore necessary to use CCD's with small pixel sizes in the range of one micron or below, which might be available in the future. With such devices even the highest spatial frequencies could be resolved, independently from the recording distance.

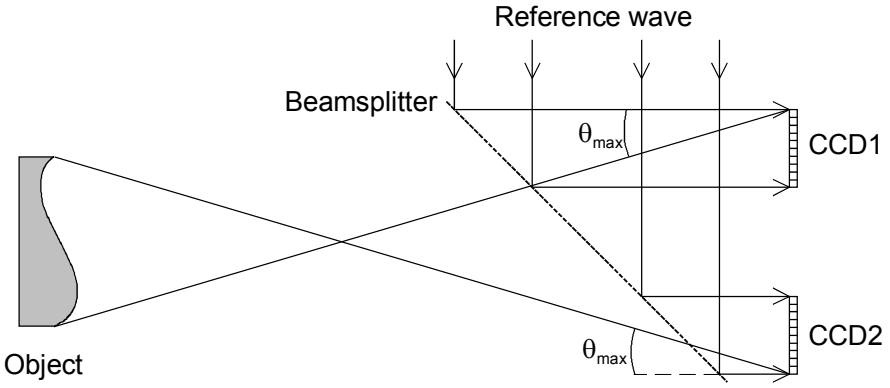

Fig. 6.21. Aperture synthesis with two CCD's